Shear Viscosity and Heterogeneous Structure of Alkylaminoethanol-Based CO_2 Absorbents

Journal:	*The Journal of Physical Chemistry*
Manuscript ID	jp-2018-00946b.R1
Manuscript Type:	Article
Date Submitted by the Author:	n/a

Complete List of Authors:	Yamaguchi, Tsuyoshi; Nagoya Daigaku Kogakubu Daigakuin Kogaku Kenkyuka, Department of Materials Process Engineering Ando, Ryuya; Nagoya Daigaku Kogakubu Daigakuin Kogaku Kenkyuka, Department of Molecular Design and Engineering Yoshida, Koji; Fukuoka University, Chemistry Yamaguchi, Toshio; Faculty of Science, Dept. of Chemistry Machida, Hiroshi; Nagoya Daigaku Kogakubu Daigakuin Kogaku Kenkyuka, Department of Chemical Systems Engineering

Shear Viscosity and Heterogeneous Structure of Alkylaminoethanol-Based CO_2 Absorbents

Tsuyoshi Yamaguchi,[1,] Ryuya Ando,[1] Koji Yoshida,[2] Toshio Yamaguchi,[2] and Hiroshi Machida[1]*

[1] Graduate School of Engineering, Nagoya University, Furo-cho, Chikusa, Nagoya, Aichi 464-8603, Japan.

[2] Department of Chemistry, Faculty of Science, Fukuoka University, Nanakuma, Jonan, Fukuoka 814-0180, Japan.

ABSTRACT

Shear viscosity of concentrated aqueous solutions of alkylaminoethanols was determined with changing the length of the alkyl chain and the concentration of dissolved CO_2. The viscosity increased with increasing the CO_2 loading, reflecting the strengthening of the intermolecular electrostatic interaction. The dependence of the viscosity on both temperature and CO_2 loading was described by a modified version of Vogel-Fulchar-Tammann equation. Compared at the same volume concentration of CO_2, the viscosity increased with increasing the alkyl chain lengths, and the dependence on the alkyl chain length increased with the CO_2 loading. At the same time, small-angle X-ray scattering exhibited the presence of a prepeak when the alkyl chain was long, and the prepeak grew with the CO_2 loading. It suggests that the presence of the heterogeneous structure increases the shear viscosity of the CO_2 absorbents when the alkyl chain is long.

1. Introduction

Reduction of the emission of CO_2 to atmosphere is crucial to prevent the global climate crisis. Although the use of renewable energies such as the solar or wind powers is desirable, the carbon capture and storage technology, called CCS, is regarded as one of the important transient technologies to reduce the CO_2 emission from the burning of fossil fuels.

CCS is a technology that removes CO_2 from the flue gases of large-scale CO_2 emitters such as power plants or iron mills and buries the captured CO_2 into deep underground. Many processes have been developed particularly for the capture of CO_2, and the use of amine-based liquid absorbent is a popular one among them.[1,2]

In the amine absorbent process, the flue gas is first contacted with the liquid absorbent containing amines. The CO_2 in the gas is dissolved into the absorbent, and stabilized through the chemical reactions with amines as[3]

$$2RR'NH + CO_2 \rightleftarrows RR'N^+H_2 + RR'NCO_2^-, \quad (1)$$

$$RR'NH + H_2O + CO_2 \rightleftarrows RR'N^+H_2 + HCO_3^-, \quad (2)$$

where R and R' stand for alkyl groups (or hydrogen atom). Only the second reaction occurs in the case of ternary amines. Provided that reactions (1) and (2) are exothermic ones, back reactions occur at elevated temperatures. The CO_2-loaded absorbent is thus heated to release CO_2, and the regenerated absorbent is recycled. The large amount of heat required for the regeneration is considered as a disadvantage of the amine absorbent process, and its reduction is highly desired.[4]

We have developed a novel phase-separation absorbent, which is composed of secondary amine, water, and polyether.[5] The three components are totally miscible at first. After the

absorption of CO_2, the absorbent is separated into two phases, namely, CO_2-rich and CO_2-lean phases, because the ionic species generated by the reactions (1) or (2) disfavors the weakly polar polyether. The single phase is recovered by the heating for regeneration. The cooperativity of the phase separation enables us to reduce the temperature difference between the absorption and the regeneration processes. By combining a heat pump, therefore, the novel phase-separation absorbent reduces the energy requirement to 1.5 GJ/ton-CO_2 (primary energy base), which is about 40 % of that of the conventional 2-aminoethanol (monoethanolamine, abbreviated as MEA) process, 4.0 GJ/ton-CO_2.[6]

The ionic species produced by the CO_2 absorption are highly concentrated in the CO_2-rich phase after the CO_2 absorption, and its ionic concentration is as high as room-temperature ionic liquids (RTILs). The shear viscosity of the CO_2-rich phase thus becomes as high as RTILs, which can be a problem for the practical application of the phase-separation absorbent.[7]

We examined absorbents with various combinations of amines and ethers, and found that the hydrophobicity of the amines and the ethers is an essential factor that control the phase behavior.[5] Changing the length of the alkyl chain of alkylaminoethanols ($C_nH_{2n+1}NHC_2H_4OH$, where n denotes the alkyl chain length) is a simple way to alter the hydrophobicity of the amine, and we demonstrated that the phase behavior varies with the alkyl chain length as expected. It is thus interesting and important question how the alkyl chain length affects the shear viscosity of the CO_2-rich phase after the CO_2 absorption.

The physicochemical properties and microscopic structure of RTILs have been studied intensively as the functions of the alkyl chain length attached to the cation. It is now well-established that RTILs with a long alkyl chain possess mesoscopic heterogeneous structure composed of polar and nonpolar domains.[8,9] Similar domain structures were also reported on

other concentrated ionic systems.[10,11,12] The strength of the domain structure of RTILs correlates with the shear viscosity, and it has been suggested that the mesoscopic domain structure may affect the shear viscosity of bulk liquids in some ways.[13] Given the similarity between RTILs and the CO_2-rich phase, we suspect that the mesoscopic domain structure also exists in the latter when the alkyl chain of the amine is long, and the mesostructure may be related to the shear viscosity of the CO_2-rich phase.

In this work, we determined the shear viscosity of concentrated alkylaminoethanol solutions with changing the alkyl chain length, the concentration of the loaded CO_2, and the temperature. The concentration of the amines was set close to that of the CO_2-rich phase of the phase-separation absorbent. An empirical equation, which is a modified version of the Vogel-Fulchar-Tammann (VFT) equation, was proposed to describe the dependence of the shear viscosity on the temperature and the CO_2 loading simultaneously. The small-angle X-ray scattering (SAXS) of the absorbents before and after the CO_2 absorption was also performed. When the alkyl chain was as long as butyl (n = 4), the prepeak representing the mesoscopic structure appeared, and it was strengthened by the CO_2 absorption. The relation between the mesostructure and the shear viscosity is discussed.

2. Experimental

We used four alkylaminoethanols ($C_nH_{2n+1}NHC_2H_4OH$), namely, 2-aminoethanol (MEA, n = 0), 2-(methylamino)ethanol (MAE, n = 1), 2-(ethylamino)ethanol (EAE, n = 2), and 2-(butylamino)ethanol (BAE, n = 4). All the amines were purchased from TCI Inc. and used

without further purification. Carbon dioxide (CO_2, > 99.95 %) was purchased from Taiyo Nippon Sanso Corporation and used as received. Distilled water was prepared with a WG203 water purification system from Yamato Scientific Co., Ltd.

The aqueous solutions of amines were prepared by weight. The initial concentration of the amines was fixed to be 80 wt%, whose amine / water ratio is close to that of the CO_2-rich phase of the phase-separation absorbent.[5] Neat CO_2 was bubbled into the solutions at 40 °C, and the concentrations of CO_2 and amines were determined. The fresh aqueous solution of the amine was then added to adjust the CO_2 loading to the target values, and the concentrations were measured again for confirmation.

The concentrations of CO_2 and amines of the solutions were determined with a TOC meter (TOC-V CPH, Shimadzu). The detailed procedure is described in literature.[5] About 0.04 g of the sample solution was diluted by distilled water up to about 40 g, and the values of total carbon (TC), inorganic carbon (IC), total organic carbon (TOC = TC – IC), and total nitrogen (TN) of the diluted solutions were measured. The background values of IC originating from the distilled water were evaluated separately, and subtracted from the values of the sample solutions. The values of TOC and TN of the distilled water were confirmed to be negligible. The concentrations of CO_2 and amines were calculated from the values of IC and TOC, respectively. It was confirmed that the latter value is consistent with that calculated from TN separately. The error of the CO_2 loading was within ±2 % in $\alpha \equiv [CO_2] / [\text{amine}]$. Since the carbamate ion, $RR'NCO_2^-$ produced in reaction (1), is decomposed into the parent amine and CO_2 during TOC measurement, the concentration of CO_2 determined in this way is the sum of those of molecular CO_2, HCO_3^-, CO_3^{2-}, and $RR'NCO_2^-$, while that of amine is the sum of those of neutral amine, protonated one, and carbamate ion.

The shear viscosity and the density of the solutions were determined using a Stabinger viscometer (SVM3001, Anton Paar). The measurements were performed at temperatures from 20 °C to 100 °C with intervals of 10 °C. The high-temperature measurements were limited by the formation of bubbles in cases of CO_2-loaded samples. The stability of the sample temperature is within ±0.002 °C, and the reproducibilities in the values of viscosity and density are within ±0.35 % and 0.1 kg/m^3, respectively, according to the specification of the viscometer.

Small-angle X-ray scattering (SAXS) measurements were performed with a Nano-Viewer small-angle X-ray diffractometer (Rigaku) using CuKα radiation (λ = 0.15418 nm). The scattering experiments were performed on both the fresh and the CO_2-loaded solutions for each amine. The concentrations of the CO_2-loaded samples are 1.7 mol/dm^3 for MEA, MAE, and EAE, and 1.8 mol/dm^3 for BAE. The volume concentrations of all the CO_2-loaded samples were set close to each other for the reasons described later. All the measurements were performed at room temperature. The range of the measured scattering vector, q, was 1.0–19.7 nm^{-1}, where q is related to the scattering angle, 2θ, as $q = (4\pi/\lambda)\sin\theta$. The scattering vector was calibrated by the measurement of silver behenate powder. The sample solution was sealed into a borosilicate glass capillary with a diameter of 1.5 mm and a wall thickness of 10 μm. The scattering intensity of the solution was obtained by subtracting the scattering intensity from the capillary after the absorption correction.

3. Results and Discussion

All the numerical values of the shear viscosity and density are tabulated in Table S1 of Supporting Information. The values of the viscosity of the aqueous MEA solution without CO_2 were in good agreement with those reported by Arachchige and coworkers.[14]

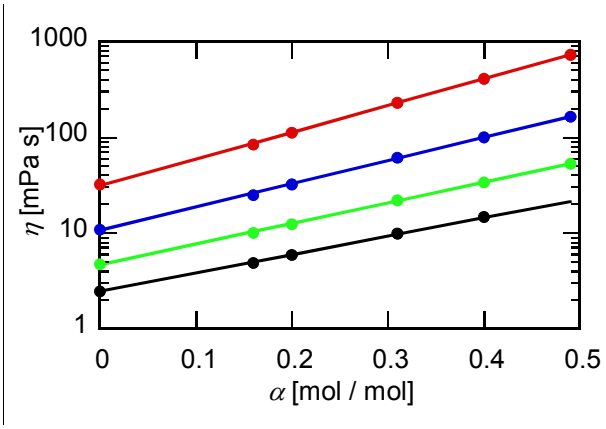

Figure 1. Shear viscosity of EAE solutions loaded with CO_2 is plotted against the molar ratio of CO_2 to EAE, $\alpha \equiv [CO_2] / [EAE]$. The temperatures of the solutions are 20 (red), 40 (blue), 60 (green), and 80 °C (black), respectively. The experimental values are shown with the filled circles, while the correlations using eq. (3) are with the solid curves.

The shear viscosity of EAE solutions at four temperatures are shown in Fig. 1 as the function of the CO_2-loading, $\alpha \equiv [CO_2] / [EAE]$. The shear viscosity increases with increasing CO_2 loading or decreasing temperature. The increase in ln η with α becomes larger at lower temperature, and it is ascribed to the increase in the intermolecular electrostatic interaction due to the production of ionic species.

Although there are two reaction schemes of the chemical absorption of CO_2 by amine, reactions (1) and (2), the former reaction is dominant when the concentration of amine is high, because a water molecule is consumed in reaction (2). We confirmed the dominance of reaction (1) in the case of EAE solutions by nuclear magnetic resonance (NMR) spectroscopy as was

performed by Yamada and coworkers.[15] The details of the experiment are described in Ref. 16, and the results are shown in Sec. S2 of Supporting Information.

The dependence of ln η on α is almost linear according to Fig. 1, which suggests the presence of a kind of ideality. If reaction (1) is exclusively dominant over reaction (2), the CO_2-loaded aqueous amine solution is regarded as the mixture of two solutions, that is, the first one is the aqueous amine solution without CO_2, and the second one is the aqueous solution of the organic salt composed of protonated amine cation and carbamate anion. The linear dependence of ln η is then regarded as an ideal mixing relation for the mixtures of the two solutions.

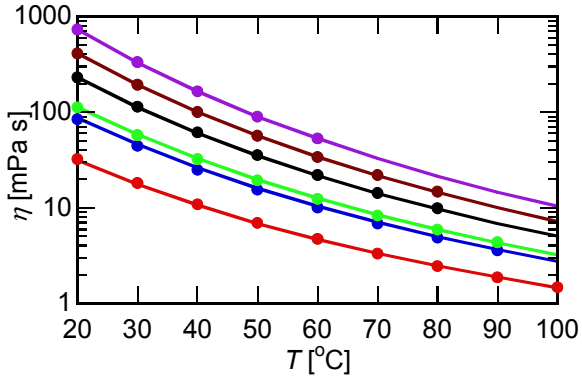

Figure 2. Shear viscosity of CO_2-loaded EAE solutions is plotted as the function of temperature, T. The values of loading, $\alpha \equiv [CO_2] / [EAE]$, are 0.00 (red), 0.16 (blue), 0.20 (green), 0.31 (black), 0.40 (brown), and 0.49 (purple), respectively. The experimental values are shown with the filled circles, while the correlations using eq. (3) are with the solid curves.

The same data on EAE solutions are plotted as the function of temperature in Fig. 2. The temperature dependence of the viscosity becomes larger on the log scale with decreasing temperature.

We shall here propose an equation to describe the dependence of the shear viscosity on α and T simultaneously. The equation below is an extension of Vogel-Fulchar-Tammann (VFT) equation that is often applied to viscous liquids including RTILs and supercooled liquids, as

$$\ln \eta(T, \alpha) = \mathrm{A} + \frac{a\alpha + b}{T - T_0}. \quad (3)$$

The details of the parameter optimization and the error estimation of the parameters are described in Sec. S3 of Supporting Information, and the results of the correlation using eq. (3) are shown in Figs. 1 and 2. Equation (3) describes the shear viscosity of EAE solutions well. Although the parameters A and T_0 can depend on α in principle, we succeeded in reproducing the experimental results keeping them constant.

The numerator of the second term of the rhs. of eq. (3) is related to the activation energy, and the ionic species produced by the CO_2 absorption increases the shear viscosity through the increase in the activation energy. The parameter T_0 of VFT equation is usually related to the glass transition temperature, and it seems rather strange that T_0 is independent of the CO_2 loading, because the glass transition is likely to occur at higher temperatures in liquids with stronger interaction. Since our experiment is limited to the temperature range far higher than T_0, however, we consider it dangerous to interpret the constant T_0 as the constant glass transition temperature.

Table 1. Parameters A, a, b, and T_0 of eq. (3) for all the amine solutions.

Amine	A [-]	a [K]	b [K]	T_0 [K]
MEA	-3.70	1026	877	162
MAE	-4.65	917	1112	153
EAE	-4.63	844	1054	162
BAE	-5.38	805	1341	140

The correlation was performed on solutions of other three amines, and the results are shown in Sec. S4 of Supporting Information. Equation (3) works well for all the amine solutions studied in this work. The root-mean-square deviation of the correlation of all the data, defined as

$$\sqrt{\frac{1}{N_{data}}\sum_{all\ data}\left\{\frac{\eta_{exp}-\eta_{cor}}{\eta_{exp}}\right\}^2}, \quad (4)$$

is 3.5 %, where N_{data} denotes the number of the data, and η_{exp} and η_{cor} stand for the experimental and correlated values of the viscosity, respectively. The parameters A, a, b, and T_0 are summarized in Table 1.

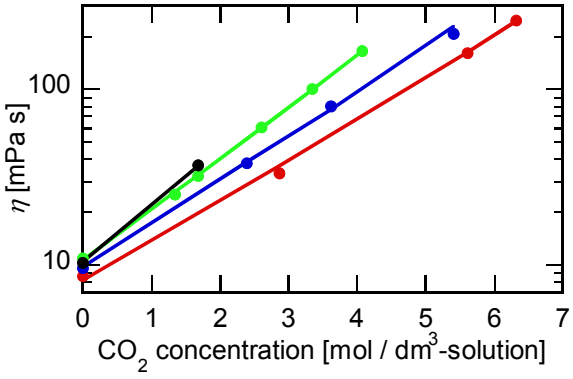

Figure 3. Shear viscosity of the solutions at 40 °C are shown as the volume concentration of the loaded CO_2. The amines are MEA (red), MAE (blue), EAE (green), and BAE (black), respectively. The experimental values are plotted with the filled circles, while the correlation by eq. (3) is with solid curves.

The shear viscosity of the four absorbents is compared at 40 °C in Fig. 3. The comparison is performed as the function of the volume concentration of the loaded CO_2 for two reasons. The first one is that the volume capacity of the absorbent is an important factor to determine the efficiencies of the process. The use of high-capacity absorbent can decrease the size of the equipment and the sensible heat required for regeneration. The second one is physicochemical.

Provided that the interionic electrostatic interaction is considered as a reason for the increase in the shear viscosity with CO_2 loading, the comparison among amines is better performed at the same number of ions in a given volume of the solution.

The shear viscosity increases with the alkyl chain length as is shown in Fig. 3, and the effect of the chain length increases with increasing the volume concentration of CO_2. The increase in the molecular size of the amine as a whole can of course lead to the increase in the shear viscosity, and the effect of the molecular size can explain the variation of the shear viscosity without CO_2. However, the increased effect of the chain length at higher CO_2 concentration cannot be ascribed simply to the molecular size.

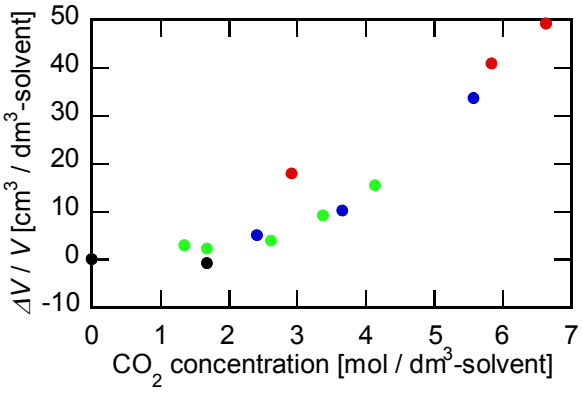

Figure 4. Relative variations of the volume of the solutions on dissolution of CO_2 at 40 °C are shown. The amines are MEA (red), MAE (blue), EAE (green), and BAE (black), respectively.

The volume expansion of the solution on CO_2 loading is exhibited as the function of the CO_2 concentration in Fig. 4. Here, the relative variation of the volume, $\Delta V / V$, is defined as

$$\frac{\Delta \mathrm{V}(n_{amine},n_{water},n_{CO2})}{\mathrm{V}(n_{amine},n_{water},0)} \equiv \frac{\mathrm{V}(n_{amine},n_{water},n_{CO2})-\mathrm{V}(n_{amine},n_{water},0)}{\mathrm{V}(n_{amine},n_{water},0)}, \quad (5)$$

where V stands for the volume of the solution, and n_{amine}, n_{water}, and n_{CO2} indicate the molar quantities of the amine, water, and CO_2, respectively. The volume expansions behave as convex

functions of the CO_2 concentration. The dissolution of small amount of CO_2 rarely accompanies the volume expansion, and the further increase in CO_2 leads to the increase in the volume of the solution. Comparing the solutions of different amines, the volume expansion is smaller in the solution of more hydrophobic amine. The smaller volume expansion means the larger reorganization of the microscopic structure to the more packed one.

The volumetric properties above can be understood in terms of the electrostriction due to the ionic species produced by reactions (1) or (2). It is well known that strong electric field of an ion leads to the contraction of surrounding solvent, which is called electrostriction. The effect of the electrostriction is stronger in less polar solvent, which explains the variation of $\Delta V / V$ in solutions of different amines. At higher concentration of ions, the electric field of an ion is shielded by surrounding other ions, and the electrostriction becomes weaker. The volume of the solution thus increase on the dissolution of CO_2 due to its van der Waals core volume.

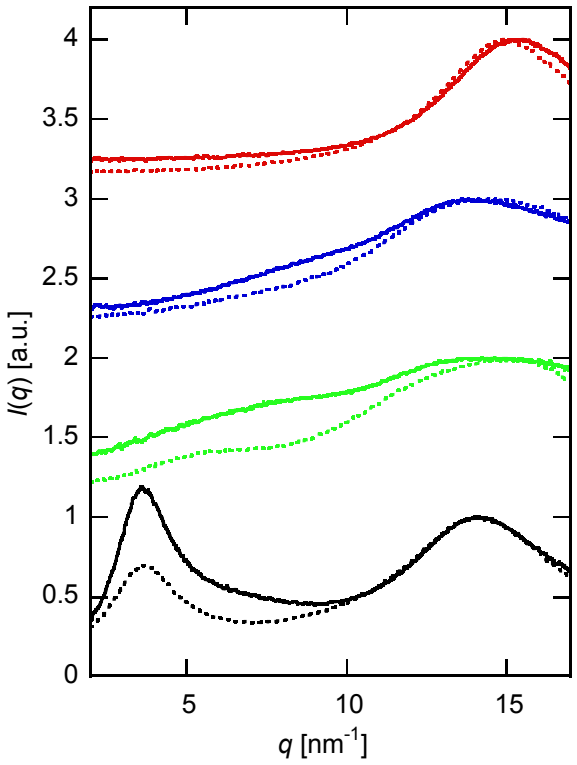

Figure 5. SAXS profile of the amine solutions before (dotted) and after (solid) CO_2 absorption are shown. The amines are MEA (red), MAE (blue), EAE (green), and BAE (black), respectively. All the profiles are normalized to the height of the respective main peaks at 13 – 15 nm^{-1}. The profiles of the solutions of different amines are shifted from each other to improve the visibility.

Figure 5 shows the SAXS profiles of all the solutions. All the profiles exhibit a peak at 13 – 15 nm^{-1}, called "main peak", which reflects the contact distance between molecules, and the height of the main peak is used as the intensity standard for normalization. In addition to the main peak, a strong peak is found at 3 nm^{-1} in cases of BAE solutions. This low-q peak is often called "prepeak". The prepeak of the BAE solution is strengthened by the CO_2 absorption, keeping the peak position constant. The EAE solution shows a broad and small shoulder around 6 nm^{-1} before the CO_2 absorption, and the shoulder is enhanced after the dissolution of CO_2. The MAE solution hardly exhibits a prepeak before CO_2 loading, but a weak shoulder is observed around 8 nm^{-1} after the CO_2 absorption. No prepeak is found in the SAXS profiles of MEA solutions before and after the CO_2 loading.

The presence of the prepeak has been reported on liquids composed of amphiphilic molecules, such as RTILs with a long alkyl chain[8,9] and higher *n*-alcohols.[17,18] The prepeak represents the mesoscopic structure composed of polar and nonpolar domains. The nonpolar domain is composed of alkyl chains. The polar domain contains the anion and the head group of the cation in the case of RTILs, while it consists of the OH groups in *n*-alcohols. The peak position of the prepeak reflects the domain size, and it increases with increasing the chain length. The prepeak of the amine solutions in Fig. 5 shifts to lower wavenumber with increasing the alkyl chain

length as are the cases of RTILs and *n*-alcohols. We thus consider that the prepeak of the amine-based CO_2 absorbent has the similar origin to those of these two classes of liquids.

The mesoscopic domain structure is formed due to the incompatibility of the polar and the nonpolar groups within a molecule. There can be two explanations for the enhancement of the prepeak on CO_2 absorption in terms of the domain structure.[19] First, given that the ionic $>N^+H_2$ and $>NCO_2^-$ groups possess higher polarity than the neutral >NH one, it is natural that the absorption of CO_2 promotes the separation of the polar and nonpolar domains. In addition, we consider that the increase in the difference of the scattering length densities between the two domains can contribute to the increase in the height of the prepeak. The loaded CO_2 dissolves into the polar domain as the $>NCO_2^-$ group in the absorbent. Since the volume expansion on CO_2 absorption is small, the volume of the polar domain experiences little change upon CO_2 loading. Therefore, the electronic density of the polar domain increases, which increases the difference in the scattering length densities of the two domains. We consider that the first mechanism is dominant, though the contribution of the second one is not negligible.

The study on the relation between the mesoscopic domain structure and the shear viscosity of bulk liquids is now in progress. Rocha and coworkers recently measured the viscosity and the SAXS profiles of two classes of imidazolium-based RTILs.[13] The first one possesses a methyl group on a nitrogen and an alkyl group on another nitrogen. The lengths of the two alkyl chains attached to the two nitrogen atoms are the same in the second one. Compared at the same total length of the alkyl chains, the former shows the stronger prepeak and the higher viscosity, and the domain structure is suggested to increase the shear viscosity.

We consider that the same mechanism works on the CO_2-loaded amine solutions studied in this work. Given that the domain structure is enhanced upon the CO_2 absorption, the effect of

the alkyl chain on the shear viscosity can be stronger with the CO_2 concentration as is exhibited in Fig. 3.

Based on the theoretical calculation using mode-coupling theory, Yamaguchi proposed two microscopic mechanisms for the domain structure to increase the shear viscosity of RTILs.[20] The first one is the direct coupling between the slow dynamics of the domain structure and the shear stress. The second one is that the microscopic dynamics within the polar domain is retarded due to the presence of the domain structure. Yamaguchi and coworkers demonstrated that the former mechanism works on higher alcohols,[21,22] while the detailed contributions of the two mechanisms are still unclear in the case of RTILs. It is thus an interesting question to clarify the detailed mechanism on the amine solutions studied in this work from the view of basic physical chemistry.

4. Summary

The shear viscosity of four alkylaminoethanol-based CO_2 absorbents is determined as the function of temperature and CO_2 loading. A modified version of the VFT equation is proposed to correlate the viscosity as the functions of these two parameters simultaneously. Compared at the same volume concentration of CO_2, the shear viscosity of the solution increases with increasing the alkyl chain length, and the effect of the chain length becomes stronger with the CO_2 loading. The SAXS profiles of these absorbents before and after the CO_2 absorption are measured. The prepeak representing the mesoscopic domain structure is observed when the alkyl chain is long, and the prepeak is enhanced by the CO_2 absorption. It is thus considered that

the mesoscopic domain structure works to increase the shear viscosity of the CO_2-loaded amine solutions, although the detailed microscopic mechanisms are to be clarified yet.

AUTHOR INFORMATION

Corresponding Author

E-mail to Tsuyoshi Yamaguchi: yamaguchi.tsuyoshi@material.nagoya-u.ac.jp

ACKNOWLEDGMENT

The ^{13}C-NMR spectrum shown in Sec. S2 of Supporting Information were measured at Chemical Instrumentation Facility, Research Center for Materials Science, Nagoya University. This work was supported by Japan Science and Technology Agency-Advanced Low Carbon Technology Research and Development Program (JST-ALCA)

Supporting Information

The Supporting Information is available free of charge on the ACS Publications website at DOI ???

Numerical values of shear viscosity and density, the ^{13}C-NMR spectrum of a CO_2-loaded EAE solution, the error estimation of the parameters in the modified version of the VFT equation, and the temperature dependence of shear viscosity of solutions with MEA, MAE, and BAE.

REFERENCES

(1) Rochelle, G. T. Amine Scrubbing for CO_2 Capture. *Science* **2009**, *325*, 1652–1654.

(2) Onoda, M.; Matsuzaki, Y.; Chowdhury, F. A.; Yamada, H.; Goto, K.; Tonomura, S. Sustainable Aspects of Ultimate Reduction of CO_2 in the Steelmaking Process (COURSE50 Project), Part 2: CO_2 Capture. *J. Sustain. Metall.* **2016**, *2*, 209-215.

(3) Vaidya, P. D.; Kenig, E. Y. CO_2−Alkanolamine Reaction Kinetics: A Review of Recent Studies. *Chem. Eng. Technol.* **2007**, *30*, 1467-1474.

(4) Goto, K.; Okabe, H.; Shimizu, S.; Onoda, M.; Fujioka, Y. Evaluation Method of Novel Absorbents for CO_2 Capture. *Energy Procedia* **2009**, *1*, 1083-1089.

(5) Machida, H.; Oba, K.; Tomikawa, T.; Esaki, T.; Yamaguchi, T.; Horizoe, H. Development of Phase Separation Solvent for CO_2 Capture by Aqueous Amine + Ether Solution. *J. Chem. Thermodyn.*, **2017**, *113*, 64-70.

(6) Machida, H.; Ando, R.; Esaki, T.; Yamaguchi, T.; Horizoe, H.; Kishimoto, A.; Akiyama, K.; Nishimura, M. Low Temperature Swing Process for CO_2 Absorption-Desorption Using Phase Separation CO_2 Capture Solvent. Submitted.

(7) Barzagli, F.; Mani, F.; Peruzzini, M. Novel Water-Free Biphasic Absorbents for Efficient CO_2 Capture. *Int. J. Greenh. Gas Control*, **2017**, *60*, 100-109.

(8) Lopes, J. N. A. C.; Pádua, A. A. H. Nanostructural Organization in Ionic Liquids. *J. Phys. Chem. B* **2006**, *110*, 3330−3335.

(9) Russina, O.; Triolo, A. New Experimental Evidence Supporting the Mesoscopic Segregation Model in Room Temperature Ionic Liquids. *Faraday Discuss.* **2012**, *154*, 97−109.

(10) Kaur, S.; Gupta, A.; Kashyap, H. K. Nanoscale Spatial Heterogeneity in Deep Eutectic Solvents. *J. Phys. Chem. B* **2016**, *120*, 6712−6720.

(11) Yamaguchi, T.; Yoshida, K.; Yamaguchi, T.; Kameda, Y.; Ikeda, K.; Otomo, T. Analysis of Prepeak Structure of Concentrated Organic Lithium Electrolyte by Means of Neutron Diffraction with Isotopic Substitution and Molecular Dynamics Simulation. *J. Phys. Chem. B*, **2017**, *121*, 5355-5362.

(12) Fujii, K.; Matsugami, M.; Ueno, K.; Ohara, K.; Sogawa, M.; Utsunomiya, T.; Morita, M. Long-Range Ion-Ordering in Salt-Concentrated Lithium-Ion Battery Electrolytes: A Combined High-Energy X-ray Total Scattering and Molecular Dynamics Simulation Study. *J. Phys. Chem. C* **2017**, *121*, 22720-22726.

(13) Rocha, M. A. A.; Neves, C. M. S. S.; Freire, M. G.; Russina, O.; Triolo, A.; Coutinho, J. A. P.; Santos, L. M. N. B. F. Alkylimidazolium Based Ionic Liquids: Impact of Cation Symmetry on Their Nanoscale Structural Organization. *J. Phys. Chem. B* **2013**, *117*, 10889-10897.

(14) Arachchige, U. S. P. R.; Aryal, N.; Eimer, D. A.; Melaaen, M. C. Viscosities of Pure and Aqueous Solutions of Monoethanolamine (MEA), Diethenolamine (DEA) and N-Methyldiethanolamine (MDEA). *Ann. Trans Nordic Rheol. Soc.* **2013**, *21*, 299−306.

(15) Yamada, H.; Matsuzaki, Y.; Goto, K. Quantitative Spectroscopic Study of Equilibrium in CO_2-Loaded Aqueous 2-(Ethylamino)ethanol Solutions. *Ind. Eng. Chem. Res.* **2014**, *53*, 1617−1623.

(16) Machida, H.; Ando, R.; Esaki, T.; Yamaguchi, T.; Norinaga, K. Modelling for CO_2 solubility in phase separation solvent. Submitted.

(17) Tomšič, M.; Bešter-Rogač, M.; Jamnik, A.; Kunz, W.; Touraud, D.; Bergmann, A.; Glatter, O. Nonionic Surfactant Brij 35 in Water and in Various Simple Alcohols: Structural Investigations by Small-Angle X-Ray Scattering and Dynamic Light Scattering. *J. Phys. Chem. B* **2004**, *108*, 7021−7032.

(18) Tomšič, M.; Jamnik, A.; Fritz-Popovski, G.; Glatter, O.; Vlček, L. Structural Properties of Pure Simple Alcohols from Ethanol, Propanol, Butanol, Pentanol, to Hexanol: Comparing Monte-Carlo Simulations with Experimental SAXS Data. *J. Phys. Chem. B* **2007**, *111*, 1738−1751.

(19) Bernardes, C. E.; Shimuzu, K.; Canongia Lopes, J. N. Comparative Structural Analyses in Four Ionic Liquid Systems: The Two Low-*q* Peaks of IL Structure Factor Functions. *Mol. Sim.* **2018**, *44*, 478-484.

(20) Yamaguchi, T. Mode-Coupling Theoretical Study on the Roles of Heterogeneous Structure in Rheology of Ionic Liquids. *J. Chem. Phys.*, **2016**, *144*, 124514.

(21) Yamaguchi, T. Viscoelastic Relaxations of High Alcohols and Alkanes: Effects of Heterogeneous Structure and Translation-Orientation Coupling. *J. Chem. Phys.*, **2017**, *146*, 094511.

(22) Yamaguchi, T.; Saito, M.; Yoshida, K.; Yamaguchi, T.; Yoda, Y.; Seto, M. Structural Relaxation and Viscoelasticity of a Higher Alcohol with Mesoscopic Structure. *J. Phys. Chem. Lett.*, **2018**, *9*, 298-301.

TOC Graphics